General Report of TC209 Offshore Geotechnics

Rapport général du TC209 Géotechnique marine

Jewell R.A.
Fugro GeoConsulting

ABSTRACT: This general report introduces the discussion session organized by ISSMGE Technical Committee 209 (TC209) "Offshore Geotechnics". The main topics include offshore wind projects, pipelines and seabed structures, seabed soils, coastal and nearshore work, and pile foundations.

RÉSUMÉ : Ce rapport général introduit la séance de discussion organisée par le Comité Technique 209 (TC209) "Géotechnique Offshore" de la SIMSG. Les principaux thèmes abordés sont les projets d'éoliennes offshore, les pipelines et structures sous-marines, les sols sous-marins, les travaux côtiers et nearshore et les fondations sur pieux

KEYWORDS: offshore, caisson, piles, pipes, cyclic load, stability diagram, lateral load, tests, numerical analysis, bearing capacity

1 INTRODUCTION.

The organizers of the 18th International Conference "Challenges and Innovations in Geotechnics" have implemented important changes to the conference format. One is the inclusion of Offshore Geotechnics at this main ISSMGE forum. Second is the focus given to the technical committees.

This general report covers the session organized by the ISSMGE Technical Committee 209 (TC209) "Offshore Geotechnics" chaired by Philippe Jeanjean. Participation by TC209 at this 18th conference includes the 2nd ISSMGE McClelland Lecture by Mark Randolph, this discussion session and a workshop on recent research and development on piles under cyclic loading.

The main difference in offshore geotechnics arises from the conditions and environment offshore. There is a stark contrast in access for site investigation, soil sampling, field testing, installation and observation. Activities offshore often require new tools. Soft soil conditions at seabed level are encountered in deepwater, frequently with high carbonate content, unusual mineralogy or biogenic activity. Combined and cyclic loading usually dominate design, whether caused by waves and currents acting on structures or by repeated expansion and contraction of pipelines on the seabed. Large displacement is a feature of the installation and operation of seabed pipelines. Many of the above features of offshore geotechnics are discussed in papers to this session.

This general report has been organized into five main subject areas: Offshore Wind; Pipelines and Seabed Structures; Seabed Soils; Coastal and Near Shore work; Pile Foundations.

Since papers on the cyclic loading of piles will be presented and discussed at the TC209 workshop, these are highlighted in this general report but will not be presented during the discussion session. The main focus for presentations will be Offshore Wind and large displacement as encountered with Offshore Pipelines.

Only a limited selection of papers will be presented at the discussion session. All the papers are in the proceedings and many will be presented at the poster session. Participants are strongly encouraged to attend the TC209 workshop where the cyclic behavior and design of piles will be presented and debated based around papers to this session.

2 OFFSHORE WIND.

2.1 *Site investigation*

Project development, engineering design and project construction are three main phases for offshore wind farms. A major challenge is to minimize geotechnical risk for foundation engineering. In current practice, geotechnical risk is addressed mainly during the engineering design phase P2 in Table 1. Ben-Hazzine and Griffiths (2013) suggest that risk management may be improved through more extensive geophysical survey and preliminary site investigation during the project development phase P1. The authors highlight various sources of geotechnical risk such as inherent soil variability, measurement errors and "transformation errors" caused by simple empirical interpretation of data.

Table 1. Timing of Geotechnical Work for Offshore Windfarms (Ben-Hazzine and Griffiths, 2013)

	Common			Proposed		
Phase	P1	P2	P3	P1	P2	P3
Desk study	X			X		
Geophysical survey		X		X		
Preliminary investigation		X		X		
Full investigation		X			X	
Assurance & validation			X			X

Phases: P1 = Development, P2 = Design, P3 = Construction

Muir Wood and Knight (2013) use experience from 15 offshore wind farm projects in the UK to illustrate the manner in which geotechnical risk was managed and to define categories of poor, mediocre and good practice (or *vice versa*).

Poor practice includes appointment of the foundation design team after site investigation is completed, insufficient planning and poor interpretation of geophysical and geotechnical surveys. Mediocre practice often involves incorrect scope for geophysical and geotechnical surveys causing extra cost and increased risk. On projects with good practice the foundation design team was appointed at the start of the project and specified the site investigation work. The ground models were

developed and refined over multiple phases of geotechnical and geophysical investigation. The authors conclude that a formal approach to risk management with staged investigations and early appointment of the foundation design team is the best practice.

2.2 *Wind turbine performance*

A wind energy project involves several disciplines within civil engineering. The complex interaction between the turbine and the supporting structure governs the dynamic behaviour. Analysis is required of the structural modal parameters that influence fatigue of a wind turbine. Indeed, continuous monitoring of modal frequencies and damping ratios during the operational life of a wind turbine can provide early warning of the onset of structural damage.

Damgaard et al. (2013) assess instrumentation data from 30 offshore wind turbines in the North Sea. The measured modal frequency and damping ratio are found to vary with time. However, the observed magnitude and pattern of change with time might result from scour erosion or backfilling around the monopile structure. This highlights that the dynamic interaction between an operating turbine and the supporting structure may be affected by changes with time of the local seabed level, something that could be reduced by scour protection.

2.3 *Foundation systems*

The power capacity of a wind turbine, typically in the range 2MW to 5MW, but increasing toward 10MW in future, determines the required height above mean sea level and the maximum horizontal and vertical loads to be supported. Deeper water increases the moment arm for both wind and wave loading and often signifies larger design storms. There are many novel features to the required foundation engineering as discussed in papers to this session, Table 2.

Table 2. Papers on Foundation Systems for Offshore Wind.

	SINGLE LOAD		CYCLIC LOAD	
Shallow Foundation	Arroyo et al	A		
Monopile			Roesen et al	E.1g; A
Caisson	Kim et al	E.c; A	Versteele et al	A
Hybrid (pile/caisson)	Arshi et al	E.1g; A		

E = Experimental (E.1g lab floor; E.c centrifuge);
A = Analysis

In brief résumé, shallow foundations and monopiles generally provide efficient support for wind turbines. However, these foundations are less effective when the moment load to be resisted increases due to larger turbines and/or deeper water. One approach is to improve the capacity by combining a monopile and shallow foundation, Figure 1. Alternatively, a caisson can support combined vertical, horizontal and moment loading at seabed level. Three or four caissons may be combined to support a structure where greater load carrying capacity is required, Figure 2.

The issues for foundation engineering discussed in the papers include: (1) the impact of the loading path and loading direction on safety factor and use of a single failure envelope; (2) improved performance by combining a shallow foundation and monopile; (3) the incremental displacement of cyclically loaded monopiles; and, (4) assessment of simultaneous pore water pressure generation and dissipation for caissons under storm loading.

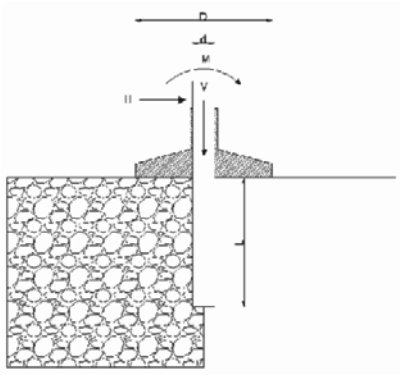

(Arshi et al, 2013)

Figure 1. Hybrid Monopile and Shallow Foundation.

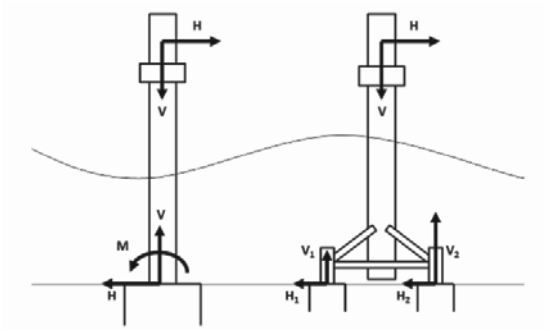

(Versteele et al, 2013)

Figure 2. Monopod and Multipod Foundations.

2.3.1 *Bearing capacity analysis*

The assessment of bearing capacity for offshore wind turbine foundations differs from onshore practice in several respects. The issues include: (a) separate correction factors in analysis for shape, depth, load inclination and eccentricity that are cumbersome and prone to calibration error; (b) use of separate partial factors on loads and resistances as in DNV-OS-J101 when the difference between favourable and detrimental effects can be subtle; and (c) simultaneous application of two major horizontal loads from wind and wave acting in separate directions. Arroyo et al highlight these issues and question the suitability of the conventional design approach for offshore wind foundations (Arroyo et al 2013).

A more satisfactory framework for capacity checks would be through failure-envelopes as detailed in the paper. Arroyo et al examine a synthetic design example to illustrate their case using the geometry of a Thornton Bank GBS and a set of derived loading parameters, Figure 3. The complex interaction between horizontal and moment loading, and the impact of different directions for wind and wave loading are illustrated by the authors using Figure 4 and the results in Table 3.

It is conventional to increase both detrimental loads at the same time, so that the load increment causing the limit to be reached is in the same direction as the reference combined load. The authors consider the cases where only wind or wave loading is increased. Such analysis might be used to assess the impact of any error in the assessment of those loads. Because of the greater influence on moment of wind loading, the analysis shows that an underestimate 21% (in this case) in the wind load would be sufficient to cause failure compared with an underestimate 50% for the wave load, Table 3.

Arroyo et al (2013) conclude that failure envelopes offer a powerful framework for analysis of shallow foundation capacity; the approach is particularly well suited for offshore wind structures that require refined design in the face of considerable uncertainty.

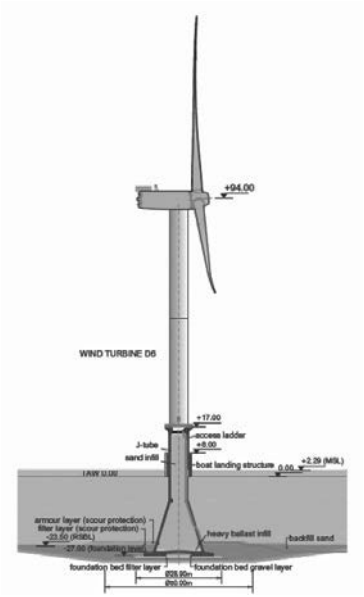

Figure 3. Thornton Bank GBS (after Peire et al 2009).

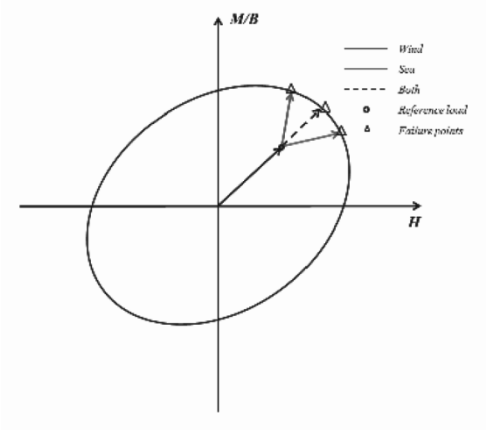

(Arroyo et al 2013)

Figure 4. Incremental loading paths to failure.

Table 3. Results of analysis on incremental load to failure.

Hypothesis	Hr (MN)	Hr / Hi	ΔH (%)
Sea	14.1	1.4	50
Both	11.6	1.15	15
Wind	10.5	1.04	21

2.3.2 *Hybrid foundations*

When considered as a monopile design, the addition of a shallow footing at seabed level may be thought of as adding "fixity" to the monopile "head" thereby generating improved resistance and stiffness to lateral loading, Figure 1. A simplified design analysis would assess the limiting moment capacity of the shallow foundation acting alone and include the equal and opposite moment resistance to the analysis of the monopile. The shallow foundation not only increases load carrying capacity but also reduces the bending moment supported by the monopile, by about 25% in the example cited by Arshi et al (2013).

Experimental modelling of these hybrid systems at 1g and in the centrifuge are described together with numerical and analytical work. The significance of the geometric ratio of footing to pile diameter, and pile length to pile diameter is demonstrated and a form for design charts proposed, Figure 5. Some tests on caisson/monopile combinations are noted and indicate additional benefit due to the lateral load resistance of the caisson. Centrifuge tests are currently underway to define better the benefit of caisson versus simple shallow foundation in such hybrid foundation systems.

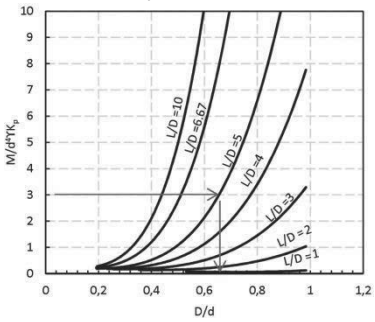

(Arshi et al 2013)

Figure 5. Moment resistance chart for hybrid foundations.

2.3.3 *Lateral displacement due to cyclic loading*

The focus above is the limit resistance of offshore wind tower foundations subject to a single application of combined loading. In practice, the structures are subject to several episodes of extreme loading caused by major storms and a great number of cycles of low amplitude loading from normal wind and wave conditions. The latter source of repeated loading may cause fatigue or serviceability problems (Roesen et al. 2013).

The authors report a series of 1g laboratory tests on monopiles in sand subject to one-way cyclic loading over more than 50,000 cycles. One limitation in these 1g tests is a more rigid pile compared with a typical prototype, but the trend of results should be similar. The cyclic loading is described by two non-dimensional ratios: the maximum moment compared with the static moment capacity $\zeta_b = \mathbf{M_{max}/M_{static}}$ in the range $1 > \zeta_b > 0$; and the ratio of the minimum to the maximum moment $\zeta_c = \mathbf{M_{min}/M_{max}}$ which has a value 1 for a static test, 0 for one-way loading (the case examined by Roesen et al) and -1 for two way cyclic loading.

The pile displacement is measured by the rotation θ at the soil surface. The results of a static load test and the measured displacement in one-way cyclic load tests ($\zeta_c = 0$) with load intensity $\zeta_b = 0.2$ to 0.4 are shown on Figure 6.

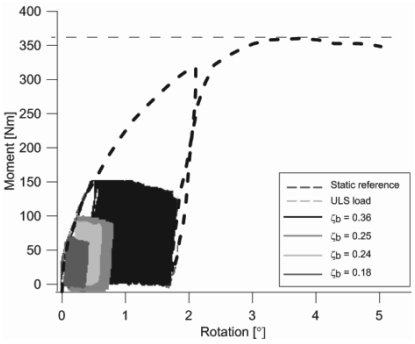

(Roesen et al 2013)

Figure 6. Static and cyclic one-way loading tests on model monopiles.

The incremental rotation due to one-way cyclic loading may be quantified with respect to the rotation caused by the first, single loading $\mathbf{\Delta\theta_N = \theta_N - \theta_1}$. Tests with different loading intensity may then be compared through the non-dimensional form $\mathbf{\Delta\theta_N/\theta_1}$ as shown on Figure 7.

The test data are compared with a simple power law $\mathbf{(\Delta\theta_N/\theta_1) = aN^b}$, where **a** and **b** are empirical constants found from testing. The power law seems to provide a reasonable asymptotic limit for the data after about 1000 or more load repetitions, Figure 7. The value of the constant **a** is found to vary almost linearly with the applied load magnitude ζ_b . The slope of accumulating displacement with repeated loading, the constant **b**, appears to be a function of the combination of

monopile and sand parameters, presumably including the installation process. The rate of accumulation appears not to depend markedly on the applied load magnitude. The analysis in §6.2 suggests that the data might also fit with a natural logarithm through to low numbers of cycles ($\Delta\theta_N/\theta_1$) = c.ln(N).

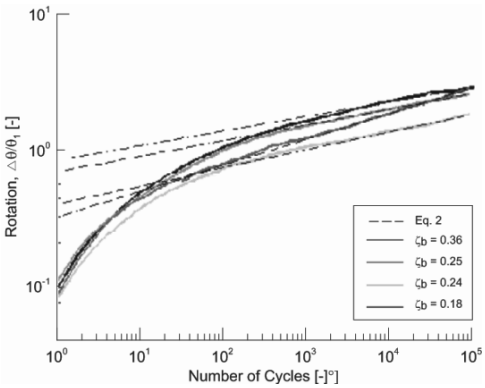

(Roesen et al 2013)
Figure 7. Monopile rotation versus number of cycles.

2.3.4 *Caisson foundations*

A centrifuge test of a caisson in sand is reported by Kim et al. (2013). The caisson response to single combined load to failure is measured and numerical analysis applied. The test details are provided elsewhere and it is not clear whether the 1/70th scale caisson was installed by suction during the centrifuge test or before testing. Soil material from the proposed site is used to model a planned prototype caisson foundation. The measured response of the modelled prototype 15.5m diameter 10.5m long caisson is shown on Figure 8 in terms of applied moment versus rotation.

The authors report a parametric analysis using FLAC to show the significant influence of the assumed elastic modulus and cohesive strength parameters assumed for the soil.

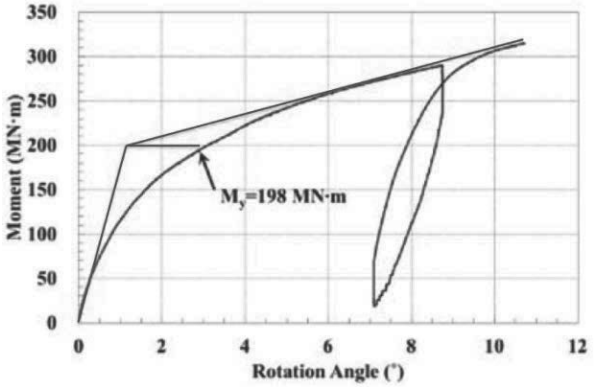

(Kim et al 2013)
Figure 8. Measured moment-rotation for prototype caisson.

The offshore design standard DNV-OS-J101 (DNV, 2011) requires structures to resist a 50 year design storm considering both peak loads and the entire history of cyclic loading. It is this latter requirement that is tackled by Versteele et al (2013) for the case of caisson foundations in sand.

Because a full analysis of cyclic loading of caissons in sand is not practically feasible with current numerical methods, the authors develop an analysis to provide insight into the competing processes of excess pore water pressure generation and dissipation during the design storm. The analysis breaks the storm into several packages of cyclic loading (magnitude, number of cycles and time). The excess pore water pressure generated at each point in the soil by the package of cyclic loading is computed analytically and input into the numerical analysis. The dissipation and redistribution of pore water pressure during the time period is computed numerically. The process is repeated for the next package of cyclic loading, and so on.

The analysis for pore pressure generation uses two relations for the sand material. First the measured cyclic shear strength versus number of cycles to liquefaction, N_l, from cyclic laboratory tests; second an empirical formula linking pore water pressure generation to number of load cycles, Figure 9. Liquefaction occurs at $u/u_{max} = 1$ when $N/N_l = 1$.

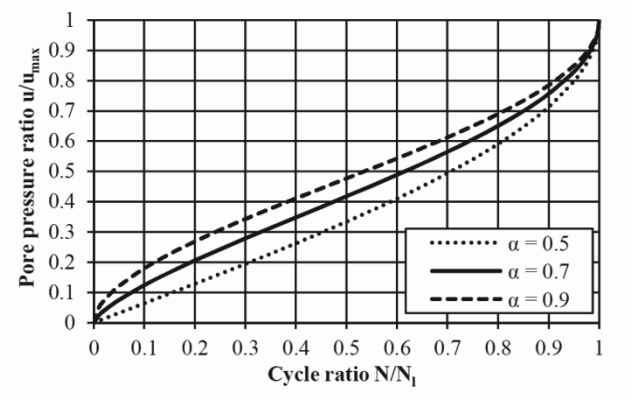

(Versteele et al 2013)
Figure 9. Generation of excess pore water pressure.

The results of a 3D analysis for a caisson foundation are reported to illustrate the method, Figure 10. The 20m diameter by 10m length caisson is subjected to a 6 hour design storm of 2160 waves. These are split for analysis into 5 individual load packages. The direction of wind and wave loading is assumed to be aligned. The results illustrate the asymmetric nature of pore water pressure generation that has potential consequences for possible differential settlement and tilting of the caisson.

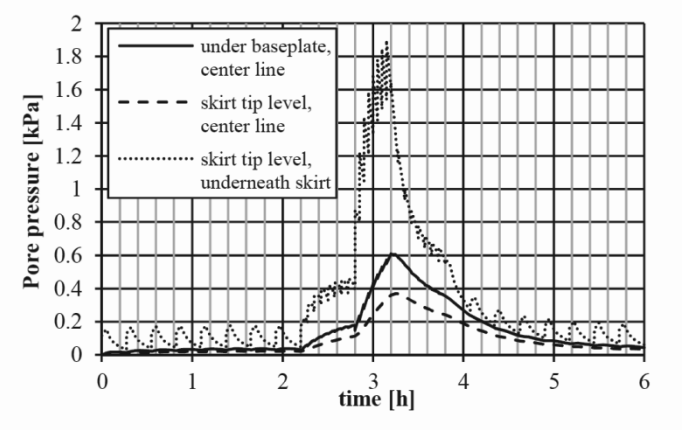

(Versteele et al 2013)
Figure 10. Example of excess pore water pressure below a caisson.

Versteele et al (2013) conclude that the model is useful in predicting areas beneath the caisson prone to the development of excess pore pressure. However, the analysis does not predict liquefaction behaviour or compute settlement, nor does it allow for load redistribution in the caisson due to the changing effective resistance in the soil during the design storm. There is further development work to be done.

3 PIPELINES AND LARGE DISPLACEMENT.

A challenging feature for offshore pipelines is the large displacement that can occur during installation and service. Large displacement is particularly extreme for laying pipe on a soft seabed. Large displacement also results from multiple cycles of heat expansion and contraction of the operating pipeline. This requires engineering design to avoid localized

pipe distortion and over-stress irrespective of the sea bed soil type. A less discussed cause of large displacement is where a pipeline crosses a seismic fault; here it is movement of the ground with respect to the pipe that causes gross distortion. Fault crossings occur both onshore and offshore.

The geotechnical analysis for large displacement requires suitable tools and numerical models and both have developed significantly in recent years. A variety of large displacement numerical methods with 3D capability are commercially available for design purposes. Similarly, constitutive models for soft clay that account for competing strain rate and strain softening effects, and competing pore pressure generation and dissipation, are available for designers. Specific numerical elements to model the large displacement interaction between a pipe and the surrounding soil are also currently under development for practical application in design (SAFEBUCK JIP). However, the constitutive and numerical modeling for large displacement in dense sand is less well advanced.

Pipe buckling and pipe walking is usually assumed to occur between fixed seabed structures. There may be scope for permitting the seabed structures to move horizontally to help accommodate axial pipe displacement.

Several of these topics are described in four papers to the discussion session.

3.1 *Dynamic embedment of offshore pipelines*

Dutta et al (2013) examine pipe laying and dynamic embedment using Coupled Eulerian Legrangian (CEL) methods available in ABAQUS software. Progressive degradation of undrained shear strength with plastic shear strain is included using the model of Einav and Randolph (2005). Similar analysis by Wang et al (2010) used remeshing and small strain (RITSS analysis).

The simplified problem is illustrated in Figure 11. A pipe is penetrated monotonically into a soft clay sea bed under self-weight (submerged weight of pipe). The pipe is then cycled laterally by a displacement u/D = ± 0.05, in the x direction of Figure 11, under constant self-weight vertical load. This causes additional pipe penetration.

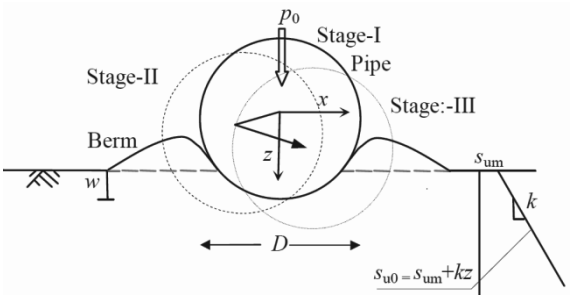

(Dutta et al 2013)
Figure 11. Pipe penetration of a seabed.

The analysis uses the same dimensions, soil parameters and loading sequence as the first stage of two pairs of centrifuge tests by Cheuk and White (2008) on a light and heavier pipe. The progressive pipe penetration and magnitude of horizontal resistance caused by cyclic lateral displacement is computed. The penetration of the pipe with cycles of lateral displacement is shown in Figure 12 for one pair of pipe tests.

Current practice is to estimate separately the embedment due to pipe laying and due to dynamic effects. The initial embedment on pipe laying involves temporary overload at the touch down point. Typically the pipe weight is increased by a "lay factor" and the initial pipe penetration under monotonic loading is computed for this higher load. The effect of small amplitude cyclic lateral motion is incorporated using a "dynamic embedment factor" that multiplies up the initial monotonic pipe lay embedment to determine a final estimated pipe embedment. The centrifuge tests and analysis here did not incorporate initial overloading of the pipe, but the forty cycles of lateral loading resulted in a dynamic embedment factor of the order 4 to 5, within the range often assumed in practice.

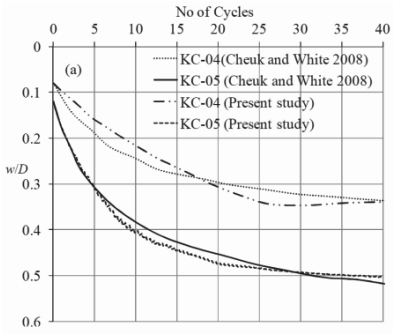

(Dutta et al 2013)
Figure 12. Static and dynamic pipe penetration of a seabed.

As shown previously by Wang et al (2010), the analysis provides insight into the size of the zone of highly sheared and softened soil around the pipe and the shape of the berms formed by pipe penetration. The results in Figure 13 are for the heavier pipe and show dynamic pipe penetration and monotonic pipe penetration to the same depth (increased vertical load). The comparison is striking. Dynamic embedment causes more extensive plastic strain softening in the soil, coloured red, and wider and flatter berms than generated by monotonic pipe penetration. The latter could be important for the analysis of initial lateral breakout of the pipe. Dynamic embedment affects the magnitude of pipe penetration, the zone of soil remoulding and the shape of the berms formed.

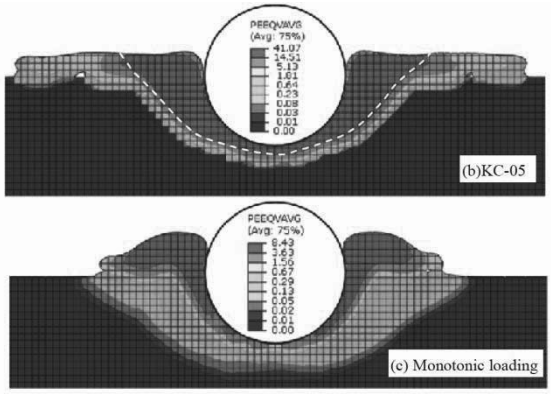

(Dutta et al 2013)
Figure 13. Dynamic and monotonic pipe penetration of a soft seabed.

3.2 *Pipeline fault crossing*

Damage is caused to pipelines that cross a seismic fault that subsequently displaces. Rupture of oil or gas pipelines can cause fire and environmental risk. For critical pipelines, the magnitude and direction of localized fault displacement should be assessed and appropriate engineering implemented to avoid pipe rupture due to ground movement.

Moradi et al completed centrifuge tests on buried steel pipe subject to an upward thrust fault at 30° to the vertical in the direction of the pipe. A fault displacement 70mm was applied across an 8mm diameter buried pipe with 0.4mm wall thickness tested in a centrifuge at 40g. In one test the pipe is simply buried in the compacted sand. A low density and light weight loose backfill was used in the second test. The axial and bending strain in the pipe was measured in both tests. The light backfill allowed the pipe to buckle and displace over a greater length considerably reducing the damage to the pipe. The pipe embedded in the sand suffered more localized deformation and damage, as illustrated by the photos post testing, Figure 14.

(Moradi et al 2013)
Figure 14. Pipe response to shear fault displacement in a centrifuge.

3.3 *Seabed structures that displace horizontally*

The sea bed in deep water is generally soft and often requires large shallow foundations to support seabed facilities. If some movement could be tolerated the size could be reduced. Further, if the structure connects with a pipeline subject to walking or other axial force, there may be merit in allowing the structure to slide horizontally to help relieve concentrated load.

Bretelle and Wallerand (2013) examine the design for a shallow foundation that displaces horizontally in a cyclic fashion, as might be caused by repeated pipe expansion and contraction. The influence of soil softening, foundation settlement and potential change in stiffness with time is examined through relatively straightforward analysis. The authors conclude that shallow foundations designed to displace horizontally could be useful for subsea pipeline networks.

3.4 *Large displacement in dense sand*

While numerical analysis for large deformation is increasingly amenable for engineering design, a relatively simple constitutive model for dense sand that provides stable large deformation analysis is still subject to study. Li et al (2013) propose a Critical State Mohr Coulomb (CSMC) model: deformation up to peak strength is elastic and thereafter dense sand dilates (including non-associated flow) and reduces in strength to the critical state angle of friction. The concept of the state parameter defined by Been and Jeffries (1985) is used.

A key objective is analysis for punch through of a spudcan footing in dense sand overlying soft clay. Li et al (2013) have not reached that target. However, development of the model starkly highlights non-uniform deformation and preferential shear band formation in dense sand post peak that makes data acquisition (lab tests) and model calibration such a challenge.

In analysis for bearing capacity of a circular plate on uniform sand, the authors found that the elastic stiffness of the sand influences bearing capacity by as much as 50% over the realistic range, reminiscent of rigidity index in penetration problems. Stiffness was found to have greater impact than dilation angle. The analysis for bearing capacity is described in terms of a combined bearing capacity factor $\mathbf{N_{q\gamma}}$ that applies across the range from $\mathbf{N_q}$ alone to $\mathbf{N_\gamma}$. The proposed formula for $\mathbf{N_{q\gamma}}$ includes soil stiffness and dilation angle along with peak friction angle, foundation size, soil unit weight and surcharge.

4 SEABED SOILS.

The three papers on soil properties cover diverse topics. Ho et al (2013) describe undrained cyclic triaxial compression tests on isotropically consolidated Singapore Marine Clay. The focus is the behavior of the clay when it is sheared monotonically to failure after cycling. The tests show that when the current mean effective stress in the sample reduces below half the original preconsolidation pressure, $\mathbf{p'/p_c'} \leq 0.5$, due to cyclic loading, some increase in mean effective stress commences at higher stress ratio in each cycle. At mean effective stress $\mathbf{p'/p_c'} \geq 0.6$ (first few cycles) the mean effective stress of the clay always reduces. This behavior is similar to normally versus over consolidated clay. The final effective stress path for monotonic triaxial compression to failure after cycling similarly depends on the mean effective stress $\mathbf{p'/p_c'}$ at the end of cycling. However, the shear strength is found to be largely independent of the previous number of load cycles and the strain amplitude.

Kim and Safdar (2013) report cyclic direct simple shear tests on compacted silty sand to define the limiting cyclic stress ratio versus number of cycles for two initial void ratios.

Tyldesley et al (2013) describe site investigation to define parameters for wind farm foundation design on a deep deposit of carbonate clayey silt till in Ontario Canada. This onshore site investigation demonstrates the use of insitu tests and shear wave velocity measurement, interpreted together with laboratory tests, to assemble knowledge on soil strength and stiffness properties.

5 COASTAL AND NEARSHORE WORK.

There are three papers on diverse topics. Madrid et al (2013) describe site investigation, cyclic laboratory tests and numerical analysis for the stability of a caisson breakwater in about 20m to 25m depth of water. The caissons are founded on a rubble mound infilling a large zone where the deep underlying soft clay soil was removed, Figure 15.

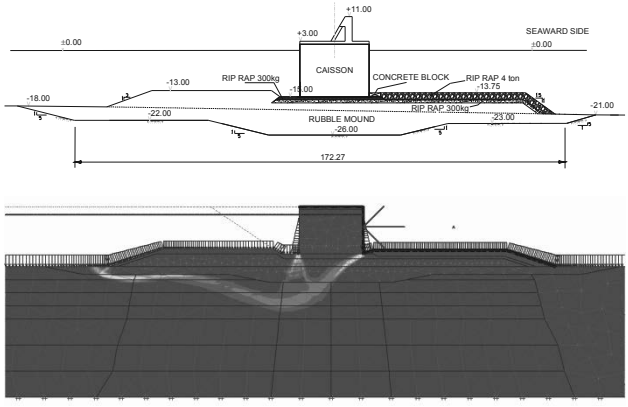

(Madrid et al 2013)
Figure 15. Caisson breakwater and stability analysis for wave impact.

There is much detail in the paper on soil testing and soil properties, loading cases for various phases of project construction and hydrodynamic testing to determine dynamic uplift. A good description is provided on the way cyclic loading and shear strength reduction were treated for design.

Relic footprints from earlier jack-up activity can occur next to the location for new shallow foundations. Ballard and Charue (2013) describe a study on a circular zone of remoulded soft clay ($\mathbf{S_r} = 2$) with a diameter equal to the size of the square mudmat and with soft clay thickness of half that size. The limiting envelope for combined moment and horizontal resistance is computed for a range of applied vertical load ($\mathbf{V/V_{ult}}$), and a range of distance between the mudmat and the remoulded zone/footprint that causes the moment and horizontal resistance to be reduced, as well as $\mathbf{V_{ult}}$. 2D and 3D analyses show very substantial benefit from the 3D geometry in this case.

A detailed design and project record for installation of large diameter, buried HDPE pipes in a nearshore environment prone to seismic loading is described by Bellezza et al (2013). Details for the case history and the various code requirements considered in design are documented. Initial measurements are provided on the vertical deflection of the installed pipes.

6 PILE FOUNDATIONS.

A lack of code guidance on capacity, stiffness and displacement for cyclically loaded piles is being addressed by collaborative research including the original GOPAL study and the current SOLCYP project, supplemented by individual research work. Several papers to this session report on SOLCYP results from instrumented field tests, calibration chamber and centrifuge

tests. SOLCYP will be presented and discussed at the TC209 workshop and recorded for publication. Therefore only some key aspects are described below to avoid duplication.

There are four axial load magnitudes: the mean $\mathbf{Q_{mean}}$ and the half-amplitude of the cyclic load $\mathbf{Q_{cyclic}}$ define the maximum $\mathbf{Q_{max} = Q_{mean} + Q_{cyclic}}$ and the minimum $\mathbf{Q_{max} = Q_{mean} - Q_{cyclic}}$ pile loads. These loads are typically referenced to the ultimate pile capacity in tension $\mathbf{Q_T}$ or compression $\mathbf{Q_{UC}}$. The ultimate capacity and the capacity under cyclic load is determined at a limiting displacement (0.1**D** or less) or due to an increasing rate of displacement; either continuing displacement after a static load increment or the cyclical displacement rate (mm/cycle).

6.1 *Stability diagram: cyclic axial loading*

The stability diagram is a non-dimensional map for cyclic pile behavior. The diagram in Figure 16 is for axial tension tests on model driven piles in dense sand in a calibration chamber (Silva et al, 2013). A similar diagram is found for the equivalent field test data (Rimoy et al, 2013). The chart defines the region of stable cyclic load combinations for a number of load cycles to be resisted. One way loading ($\mathbf{Q_{mean}}$>$\mathbf{Q_{cyclic}}$) is more stable. The dashed line shows the limit of valid load combinations.

Puech et al (2013) provide the equivalent stability diagrams for cyclic compression loading of bored piles in dense sand from field and centrifuge tests. The field tests by Benzaria et al (2013a) are shown on Figure 17. The results from centrifuge model tests are very similar. Note that only one-way loading was tested and the data should not be extrapolated beyond.

While bored piles in stiff clay have lower ultimate resistance compared with driven piles, cyclic compression tests on bored piles in over-consolidated clay indicate a much larger range of stable load combinations compared with piles in dense sand (Benzaria et al, 2013b).

Information on deformation can be included on the stability diagram as shown by Rimoy et al (2013) for field tests under cyclic axial tension on driven piles in sand, Figure 18. The data on the accumulation of displacement with cycling shows mostly stable behavior that suddenly degrades near the limiting number of cycles, a rather "brittle" behavior under tensile load.

A consistent observation for driven piles in dense sand is that stable cycling increases the ultimate capacity when tested subsequently. This is attributed to densification with some relaxation in lateral effective stress around the pile, as measured in the exceptional data of Silva et al. (2013). Conversely, strong cyclic loading (as would lead to instability) acts to reduce the ultimate axial pile capacity that can be mobilized subsequently.

Data on large axial pile tests in silt on a 4.2m long test pile are also interpreted in a stability diagram by Chen et al (2013).

6.2 *Cyclic lateral loading*

Rosquoët et al (2013) report data on lateral displacement for model driven piles in sand tested under one-way loading at 40g in a centrifuge. As in §2.3.3, but for displacement rather than rotation, the lateral displacement $\mathbf{y_N}$ compared with the first load displacement $\mathbf{y_1}$ [$\mathbf{\Delta y_N = y_N - y_1}$] is linked with the number of cycles. A logarithmic form $\mathbf{\Delta y_N / y_1 = c.ln(N)}$ fits the data well where **c** varies with the amplitude of cyclic load and the maximum lateral load (equivalent to $\mathbf{2Q_{cyclic}/ Q_{max}}$ in the axial terminology above, written as **DF/F** by Rosquoët et al). Based on their test data the authors suggest $\mathbf{c = 0.1(DF/F)^{0.35}}$ as a general fit, but sand and pile properties might also be important.

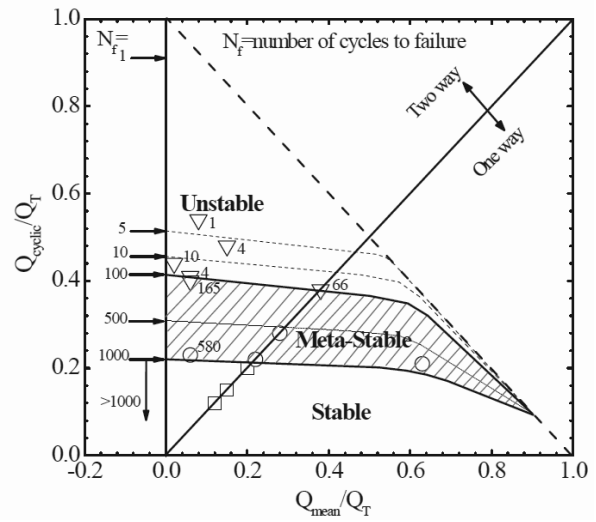

(Tsuha et al (2012) calibration chamber tests)
Figure 16: Stability diagram: tension tests on model driven piles in sand.

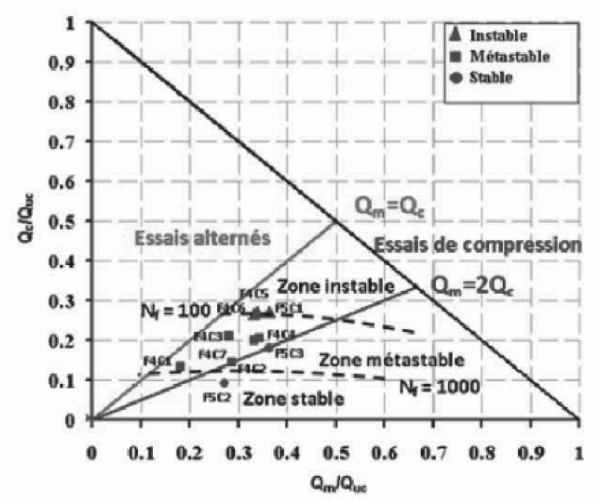

(Puech et al, 2013)
Figure 17: Stability diagram: field compression on bored piles in sand.

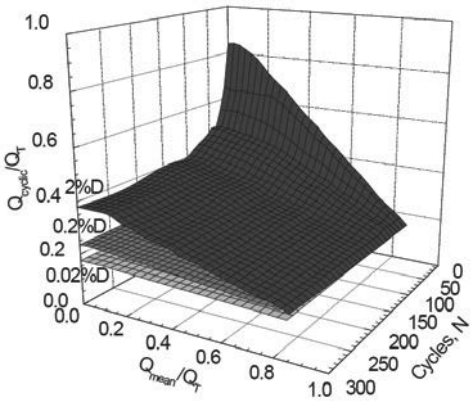

(Rimoy et al, 2013 field tension tests on driven piles in sand)
Figure 18: Stability diagram: accumulated displacement.

The natural logarithm form has the advantage of fitting the data through to low numbers of cycles (recall §2.3.3). Rosquoët et al (2013) also note that the maximum moment in the pile does not increase significantly with lateral cyclic loading. Finally, the work to extend **p-y** analysis for laterally loaded piles failed to capture the measured behavior beyond the first few cycles.

6.3 *Extension of t-z analysis to cyclic loading*

Burlon et al (2013) extend static **t-z** analysis for piles in sand to the case of tensile and compressive cyclic load and compare the results with centrifuge test data. The analysis turns out not yet to be practical as four new parameters are introduced that require measurement in cyclic pile tests. Even then, the fit with the test data is good only for relatively few load cycles.

6.4 *Plugging of open-ended displacement piles*

Laboratory tests on sand to measure pile plugging, using PIV observations, are described by Lueking and Kempfert (2013). The fully plugged limit IFR=0 was not achieved in the tests. The results of 2D Plaxis analysis are reported to investigate the mechanism of plugging. Based on this study, the authors propose two largely empirical calculation methods for the analysis of end-bearing for open-ended, partially plugged piles.

6.5 *Cyclic pressuremeter tests*

Reiffsteck et al (2013) report new work on the application of Ménard and self-boring pressuremeter tests to measure the change in soil properties with cyclic loading and, potentially, liquefaction resistance. Data are reported for several sites where cyclic pile tests were completed (SOLCYP). The authors emphasise the importance of a high quality borehole and the need for at least 50 cycles of repeated load to characterize the shear modulus. Soil horizons susceptible to liquefaction could be identified by large volume expansion. The acquisition of pore water pressure data during the test would greatly improve the test control (data on drainage/rate effects) and interpretation.

6.6 *Osterberg cell testing*

The general reporter is not aware of recent cyclic pile tests using O-Cell technology (Osterberg, 1989). A two level O-Cell test arrangement, for example, permits end bearing to be eliminated from cyclic axial compression tests on piles.

7 CONCLUSIONS.

As demonstrated by papers to this session, the practical challenges of offshore geotechnics actively drive forward the development of soil mechanics and geotechnical engineering. This is partly due to more extreme loading and deformation than usually encountered onshore. The fruits of this research and development are of great value for the overall understanding and pactice of geotechnical engineering. That is why offshore geotechnics should remain part of this key ISSMGE conference.

8 ACKNOWLEDGEMENTS

The author would thank TC209 Chairman Philippe Jeanjean for the invitation to prepare this General Report, and colleagues J.C. Ballard, P. Peralta and V. Whenham for valuable support.

9 REFERENCES

Arroyo M., Abadias D., Alcoverro J. and Gens, A. 2013. Shallow foundations for offshore wind towers. *Proc. 18th ICSMGE,* Paris.

Arshi H.S., Stone K.J.L., Vaziri M., Newson T.A., El-Marassi, M., Taylor R.N. and Goodey R.J. 2013. Modelling of monopile-footing foundation system for offshore structures in cohesionless soils. *Proc. 18th ICSMGE,* Paris.

Ballard J.C. and Charue N. 2013. Influence of jack-up footprints on mudmat stability - How beneficial are 3D effects? *Proc. 18th ICSMGE,* Paris.

Been, K. and Jefferies, M.G. (1985). A state parameter for sands. Géotechnique, Vol. 35(2), pp. 99-112.

Bellezza I., Mazzieri F., Pasqualini E., D'Alberto D. and Caccavo C. 2013. Design and installation of buried large diameter HDPE pipelines in a coastal area. *Proc. 18th ICSMGE,* Paris.

Ben-Hassine J. and Griffiths D.V. 2013. Geotechnical Exploration for Wind Energy Projects. *Proc. 18th ICSMGE,* Paris.

Benzaria O., Puech A. and Le Kouby A. 2013a. Essais cycliques axiaux sur des pieux forés dans des sables denses. *Proc. 18th ICSMGE*.

Benzaria O., Puech A. and Le Kouby A. 2013b. Essais cycliques axiaux sur des pieux forés dans l'argile surconsolidée des Flandres. *Proc.18th ICSMGE,* Paris.

Bretelle S., Wallerand R. Fondations Superficielles Glissantes pour l'Offshore Profond – Méthodologie de Dimensionnement. *Proc. 18th ICSMGE,* Paris.

Burlon S., Thorel L. and Mroueh H. 2013. Proposition d'une loi t-z cyclique au moyen d'expérimentations en centrifugeuse. *Proc. 18th ICSMGE,* Paris.

Chen R.P., Ren Y., Zhu B. and Chen Y.M. 2013. Deformation behavior of single pile in silt under long-term cyclic axial loading. *Proc. 18th ICSMGE,* Paris.

Cheuk, Y.C. and White, J.D. (2008). Centrifuge modelling of pipe penetration due to dynamic lay effects. Proc. Int. Conf. on Offshore Mechanics and Arctic Engineering, Portugal. OMAE2008-57923.

Damgaard M., Andersen J.K.F., Ibsen L.B. and Andersen L.V. 2013. Time-Varying Dynamic Properties of Offshore Wind Turbines Evaluated by Modal Testing. *Proc. 18th ICSMGE,* Paris.

DNV-OS-J101 (2011). Design of Offshore Wind Turbine Structures. Det Norske Veritas (DNV) Offshore Standard, September 2011.

Dutta S., Hawlader B. and Phillips R. 2013. Numerical investigation of dynamic embedment of offhore pipelines. *Proc. 18th ICSMGE*.

Einav, I. and Randolph, F.M. (2005). Combining upper bound and strain path methods for evaluating penetration resistance. Int. J. Numer.Meth. Engng., Vol. 63, pp. 1991-2016.

Ho J., Goh S.H. and Lee F.H. 2013. Post Cyclic Behaviour of Singapore Marine Clay. *Proc.18th ICSMGE,* Paris.

Kim D.J., Youn J.U., Yee S.H., Choi J., Choo Y.W., Kim S., Kim J.H., Kim D.S. and Lee J.S. 2013. Centrifuge test and numerical modelling for a suction bucket monopod foundation. *Proc. 18th ICSMGE,* Paris.

Kim J.M. and Safdar M. 2013. Behaviour of marine silty sand subjected to long term cyclic loading. *Proc. 18th ICSMGE,* Paris.

Li X., Hu Y. and White D. 2013. A large deformation finite element analysis solution for modelling dense sand. *Proc. 18th ICSMGE*.

Lueking J. and Kempfert H.-G. 2013. Plugging Effect of Open-Ended Displacement Piles. *Proc. 18th ICSMGE,* Paris.

Moradi M., Galandarzadeh A. and Rojhani M. 2013. The new remediation technique for buried pipelines under permanent ground deformation. *Proc. 18th ICSMGE,* Paris.

Muir Wood A. and Knight P. 2013. Site investigation and geotechnical design strategy for offshore wind development. *Proc.18th ICSMGE*.

Osterberg, J.O. 1989. New Device for Load Testing Driven Piles and Drilled Shafts Separates Friction and End Bearing. Proc. Int. Conf. on Piling and Deep Foundations, London, A.A. Balkema, p. 421.

Peire, K., Nonneman, H. & Bosschem E. (2009) Gravity Base Foundations for the Thornton Bank Offshore Wind Farm. Terra et Aqua, No. 115, pp. 19–29

Puech A., Benzaria O., Thorel L., Garnier J., Foray P., Silva M. and Jardine R. 2013. Diagrammes de stabilité cyclique de pieux dans les sables. *Proceedings 18th ICSMGE,* Paris.

Reiffsteck P., Fanelli S., Tacita J.L., Dupla J.C. and Desanneaux G. 2013. Utilisation des essais d'expansion cyclique pour définir des modules élastiques en petites déformations. *Proc. 18th ICSMGE*.

Rimoy S., Jardine R. and Standing J. 2013. Displacement response to axial cyclic loading of driven piles in sand. *Proc. 18th ICSMGE*.

Roesen H.R., Ibsen L.B. and Andersen L.V. 2013. Experimental Testing of Monopiles in Sand Subjected to One-Way Long-Term Cyclic Lateral Loading. *Proc. 18th ICSMGE,* Paris.

Rosquoët F., Thorel L., Garnier J. and Chenaf N. 2013. Pieu sous charge latérale : Développement de lois de dégradation pour prendre en compte l'effet des cycles. *Proc. 18th ICSMGE,* Paris.

Silva M., Foray P., Rimoy S., Jardine R., Tsuha C. and Yang Z. 2013. Influence des chargements cycliques axiaux dans le comportement et la réponse de pieux battus dans le sable. *Proc. 18th ICSMGE*.

Tyldesley M., Newson T., Boone S. and Carriveau R. 2013. Characterization of the geotechnical properties of a carbonate clayey silt till for a shallow wind turbine foundation. *Proc. 18th ICSMGE*.

Versteele H., Stuyts B., Cathie D. and Charlier, R. 2013. Cyclic loading of caisson supported offshore wind structures in sand. *Proc.18th ICSMGE,* Paris.

Wang, D., White, D. J. and Randolph, M. F. (2010). Large deformation finite element analysis of pipe penetration and large-amplitude lateral displacement. Canadian Geotech. Jrnl, Vol. 47, pp. 842-856.